Science of the Total Environment 612 (2018) 1506–1515

Contents lists available at ScienceDirect

Science of the Total Environment

journal homepage: www.elsevier.com/locate/scitotenv

Air pollution at Rochester, NY: Long-term trends and multivariate analysis of upwind SO_2 source impacts

Fereshteh Emami [a,1], Mauro Masiol [a,b], Philip K. Hopke [a,b,*]

[a] Center for Air Resources Engineering and Science, Clarkson University, Potsdam, NY 13699, United States
[b] Department of Public Health Sciences, University of Rochester School of Medicine and Dentistry, Rochester, NY 14642, United States

HIGHLIGHTS

- PM2.5, major species and gaseous pollutants are analyzed over 15 years (2001–2015).
- Trends are estimated trough Mann-Kendall tau-Sen's slope and piecewise regression.
- Impacts of changes in fuel sulfur content and power plant emissions are pointed out.
- Regional sources of sulfate are related to state-wide changes in SO2 emissions.
- The feedback of past mitigation strategies and action plans in U.S. is discussed.

GRAPHICAL ABSTRACT

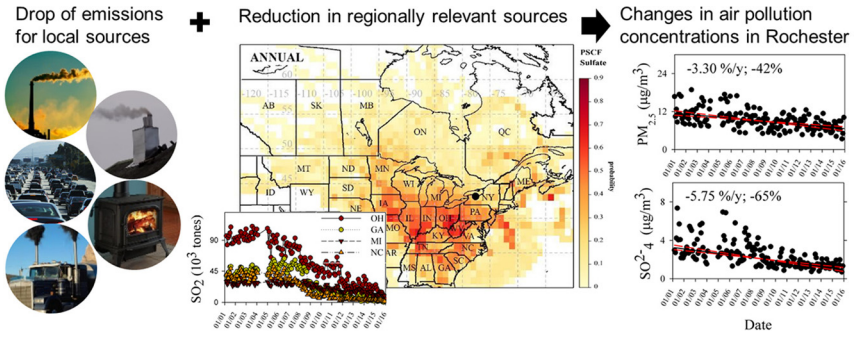

ARTICLE INFO

Article history:
Received 9 July 2017
Received in revised form 23 August 2017
Accepted 4 September 2017
Available online xxxx

Editor: D. Barcelo

Keywords:
Air pollution
Trends
Local sources
Regional sources
Mitigation policies
Northeast United States
Multivariate analysis

ABSTRACT

There have been many changes in the air pollutant sources in the northeastern United States since 2001. To assess the effect of these changes, trend analyses of the monthly average values were performed on $PM_{2.5}$ and its components including major ions, elemental carbon (EC), organic carbon (OC), and gaseous pollutant concentrations measured between 2001 (in some cases 1999) and 2015 at the NYS Department of Environmental Conservation sites in Rochester, NY. Mann-Kendall regression with Sen's slope was applied to estimate the trends and seasonality. Using piecewise regression, significant reductions in the air pollution of Rochester area were observed between 2008 and 2010 when a 260 MW coal-fired power plant was decommissioned, new heavy-duty diesel trucks had to be equipped with catalytic regenerator traps, and the economic recession that began in 2008 reduced traffic and other activities. The monthly average $PM_{2.5}$ mass showed a downward trend (-5 μg/m^3; -41%) in Rochester between 2001 and 2015. This change is largely due to reductions in particulate sulfate that showed a 65% decrease. The sulfate concentrations were compared to changes in SO_2 emissions in seventeen upwind source domains, and other systematic changes by multivariate linear regression. Selectivity ratio obtained from target projection discriminated the most important source domains that are SO_2 emissions from Georgia for winter, North Carolina for transition (spring and fall) and Ohio along with other influences for summer. North Carolina and Michigan were identified as the main sources for entire period. These observations suggest that any further reductions in the specified regional SO_2 emissions would result in a proportional decrease in sulfate in Rochester.

* Corresponding author at: Center for Air Resources Engineering and Science, Clarkson University, Potsdam, NY 13699, United States.
E-mail address: phopke@clarkson.edu (P.K. Hopke).
[1] Current Address: Department of Physics & Chemistry, Southeastern Louisiana University 10878, Hammond, LA 70402, United States.

http://dx.doi.org/10.1016/j.scitotenv.2017.09.026

1. Introduction

Exposure to air pollution produces increased risks for many adverse human health outcomes (Adam et al., 2015; Franklin et al., 2015; Katsouyanni et al., 2009; Maynard, 2009; Straif et al., 2013). Deteriorating air quality also directly and indirectly affects the climate (Seinfeld and Pandis, 2016), impairs visibility (Hyslop, 2009) and may contribute to damage materials and cultural heritage objects (Watt et al., 2009). According to the World Health Organization (WHO, 2016), urban air pollution concentrations have increased globally by 8% from 2008 to 2013. Developed countries have generally experienced an improvement in air quality (Fenger, 2009). For example, declines in ambient concentrations of many air pollutants have been measured over the past several decades in North America and Europe because of legislative efforts, implementation of successful mitigation policies, and through the application of best control technologies (Colette et al., 2011; Parrish et al., 2011).

In the United States, National Ambient Air Quality Standards (NAAQS) set limit values to be attained for air pollutants considered harmful to public health. The attainment of NAAQS requirements is monitored through a network of sampling stations managed by state, local, and tribal agencies. Beyond its regulatory role, the data collected at these sites represent a valuable resource for providing the information necessary to develop and implement strategies for further improving air quality. In addition, the long-term historic data can be used to assess the changes observed over time and the positive/null/negative effects of the mitigation measures adopted at local, national, and even international scales.

This study analyzes 15 years of air pollution data measured in Rochester, NY, a city that can be taken as representative of typical medium-sized cities in northeastern United States. During the 2001/15 period, the study area underwent major changes in emissions, including the reduction of sulfur content in highway and non-road diesel fuel and then distillate oils used for domestic/commercial heating (No. 2 oil), the closure of a large coal-fired power plant, the reduction of local industrial emissions, and increases in residential wood combustion. In addition, changes of emissions and concentrations of air pollutants over the entire eastern U.S. have been reported (Brown-Steiner et al., 2016; Dallmann and Harley, 2010; Duncan et al., 2016; Frost et al., 2006; Hogrefe et al., 2004; Nopmongcol et al., 2016; Pye et al., 2009; Tagaris et al., 2007). Thus, the analyses of temporal trends provide opportunities to examine the influence of these changes in sources on the local and regional scale.

A series of air pollutants measured at three urban sites in Rochester, NY between 2001 and for some, back to 1999 and 2015 were analyzed in this study, including carbon monoxide (CO), ozone (O_3), sulfur dioxide (SO_2), black carbon (BC), and PM with aerodynamic diameter <2.5 μm ($PM_{2.5}$). $PM_{2.5}$ data also include their chemical speciation for major inorganic ions (nitrate, sulfate, K^+), carbonaceous fractions (organic and elemental carbon: OC, EC) and elemental composition. The relationships among air pollutant species were investigated to examine their interrelationships and potential environmental implications. Finally, measured concentrations are regressed against the measured SO_2 emissions from upwind source areas. These results assess the effects of previously adopted mitigation measures, changes in emissions in the NE U.S, and may suggest the implementation of future air quality mitigation strategies in New York State (NYS).

2. Materials and methods

2.1. Study area and potential sources

Rochester lies on the southern shore of Lake Ontario and is the third most populous city in New York State (approximately 210,000 inhabitants in the 2010 Census), but its metropolitan area includes >1 million inhabitants. Rochester also lies ~100 km ENE of Buffalo (metropolitan area with 1.1 million inhabitants) and ~150 km SSW of Toronto (~2.6 million inhabitants). Its climate is typical of the northeastern United States with temperate summers and cold winters (average −18 °C) with significant snow (~250 cm per year) due to the occasional lake effect storms.

The emissions in Rochester include typical diffuse urban sources with only a few industrial sources. Intense road traffic is present across the urban major routes carrying traffic to and from downtown (e.g., route 96) as well as Interstate Highways I-90, I-490 and I-590. Traffic volumes into the city were relatively constant during 2001/15 based on the annual average daily traffic estimations for selected roads provided by NY Department of Transportation (Fig. SI1, Supplementary information). Engine controls and after treatment technologies have reduced exhaust emissions including CO, NO_x, and PM. Changes in emissions from in-use gasoline and diesel vehicles have been reported in prior studies (Bishop et al., 2011; Bishop and Stedman, 2008; Maricq, 2007; May et al., 2014; McDonald et al., 2013). In addition, the implementation of the highway diesel fuel sulfur requirements as part of the 2007 Heavy-Duty Highway Rule (https://www3.epa.gov/otaq/highway-diesel/) resulted in the nationwide transition of on-road diesel fuels from low sulfur diesel (<500 ppm) to ultra-low sulfur diesel (<15 ppm) in 2006/7. As of July 1, 2007, all new heavy-duty diesel trucks must have particle control traps and as of January 1, 2010, NO_x controls must also be implemented on all new heavy-duty diesel vehicles. EPA mandated the sulfur content to not exceed 500 ppm effective June 2007 for nonroad locomotive and marine (NRLM) diesel fuels and <15 ppm (ultra-low sulfur diesel) effective June 2010 for nonroad fuel, and June 2012 for locomotive and marine fuels (DieselNet, 2017). In New York State, all No. 2 oil sold for any purpose including building heating, on-road and off-road fuels, after July 1, 2013 must be ultralow sulfur.

Natural gas is the primary fuel in the city for domestic and commercial heating. Estimations for the whole Monroe County (NYSERDA, 2016) reported that ~80% of housing units used natural gas and 1.5% bottled LPG in 2009/13. However, Wang et al. (2011a, 2012a, 2012b) reported that wood combustion sources contributed up to ~30% of $PM_{2.5}$ mass measured at Rochester in winter. Residential wood combustion is a renewable alternative to natural gas. It was estimated that housing units burning wood for space heating fuel increased from 1475 in 2000 (NYSERDA, 2009) to 2035 in 2009/13 (NYSERDA, 2016). However, most wood combustion is recreational and done on weekends.

At the start of this period, two large facilities largely dominated the industrial emissions. A large coal-fired power plant (capacity of 260 MW) located on the shores of Lake Ontario (~12 km N of downtown Rochester) was a major source of SO_2 and ultrafine particles (Kasumba et al., 2009; Wang et al., 2011b, 2012a, 2012b). It was shut down beginning in February 2008 and completed at the end of April 2008. A coal-fired cogeneration plant (Eastman Kodak complex) located in a suburban area (~6 km NW from downtown) was another source of SO_2 and particles. Its production decreased during recent years following the transition from film to digital cameras.

Other sources may be present in the area, such as off-road transport (i.e. diesel rail, shipping on Lake Ontario to the Port of Rochester, emissions from the airport), and other non-road sources (i.e., diesel construction equipment). Regional transport of polluted air masses from Ontario, the Ohio River Valley, and the eastern coast of the United States can also affect air quality.

2.2. Data sources

Air quality data used in this study were collected at three NYS Department of Environmental Conservation (NYS DEC) sites in Rochester. From 2001 to April 2004, air pollution concentrations were measured in downtown Rochester (USEPA site code 36-055-6001: 46.16 N, 77.6 W, 160 m a.s.l.) and on the eastern side of the city (USEPA Site code 36-055-1004: 43.165512 N, 77.554511 W, 130 m a.s.l.). The downtown

site was on the roof of the central fire headquarters (~10 m in height), which lies approx. 100 m south of a high-volume traffic road (Inner Loop, ~86,000 vehicles day^{-1}). The other site was in a trailer placed in a residential neighborhood on the eastern side of the city. In May 2004, the sampling sites were consolidated and moved to NYS DEC Rochester2 site (USEPA site code 36-055-1007: 43.15N, 77.55W, 137 m a.s.l.) that lies ~300 m from the intersection of two major highways (I-490 and I-590) with an average traffic of ~230,000 vehicles day^{-1} (Fig. SI2).

Hourly gaseous and $PM_{2.5}$ data from automatic monitors and every third day $PM_{2.5}$ and $PM_{2.5}$ chemically speciated data (filter-based) were retrieved from the EPA Air Quality System (AQS) (www.epa.gov/aqs). Hourly pollutant concentrations were measured using EPA equivalent or reference methods: CO with ultra-sensitive gas filter correlation analyzers based on nondispersive infrared spectroscopy; O_3 with ultraviolet absorption; SO_2 with pulsed fluorescence technology analyzers; $PM_{2.5}$ was measured hourly with a heated tapered element oscillating microbalance (TEOM). A non-linear Julian Day based adjustment was.

applied to the TEOM data to remove the seasonal bias. It provides approximate comparability the Federal Reference Method (FRM) values. Felton (2005) and Schwab et al. (2006) describe this correction in detail. In addition, black carbon (BC) was measured with aethalometer. Beginning in July 2008, a 2-wavelength aethalometer (Magee Scientific Model AE22) was deployed, allowing the calculation of Delta-C (DC), i.e. the difference between absorbance at 370 and 880 nm. Delta-C has been shown to be a marker for biomass burning emissions (Rattigan et al., 2013), particularly in Rochester (Wang et al., 2012a).

Filter-based samples chemical speciation network (CSN) were collected every third day as part of the EPA Speciation Trends Network (now the Chemical Speciation Network) and analyzed for elements by x-ray fluorescence (XRF), elemental carbon (EC) and organic carbon (OC) by thermo-optical analysis, and major inorganic ions (K^+, nitrate, sulfate) by ion chromatography. Details of the speciation trends network (STN) and CSN sampling network, analyses, and quality assurance are provided by Solomon et al. (2014).

Measured SO_2 emissions data for northeastern North America were retrieved from (i) the EPA Air Markets Program Data for U.S. (USEPA, 2017), and (ii) the Environment Canada Air Pollutant Emission Inventory (APEI) for Ontario (ECCC, 2017).

2.3. Consistency of dataset and data processing

Data are validated by NYS DEC before submission to the EPA AQS, but were examined further to ensure a robust and reliable dataset. Concentrations below the detection limits (DL) were set to DL/2. Since 24-h data provided by CSN Network are provided without correction for measured blanks or artifact values (Solomon et al., 2014), a series of data processing procedures were performed. All species were corrected for the blank values provided by EPA, except for the OC. Positive and negative artifacts in the sampling of OC on quartz fiber filters are due to the evaporation/absorption of semivolatile organic compounds in the filter media prior, during and/or after the sampling (Chow et al., 2010; Dillner et al., 2009). Various methods have been proposed to compensate for OC artifacts (Watson et al., 2009). Since a standard method has not been promulgated and only limited blank data are available for OC from EPA to account for field, trip, and backup filter, OC blank values were estimated using the approach of Kim et al. (2005), i.e. using the intercept of a linear regression of $PM_{2.5}$ against OC concentrations. Since there was a change in the OC/EC protocol in the EPA Chemical Speciation Network in April 2009 (Solomon et al., 2014), blank corrections were made separately using all of the available data before and after the change in the analytical protocol.

A key factor in reliably estimating long-term trends is to have a consistent dataset over the entire study period. However, several major changes in sampling locations and analytical methods occurred during the 2001 to 2015 period. Thus, adjustments were made as follows:

- The site location changed in 2004. Although there is a moderate distance (~4.8 km) between the downtown site and the new east side site, it can be assumed that the two sites are affected by similar mobile sources (road traffic) and area sources (domestic heating) typical of densely inhabited urban environments. Road traffic is widespread in Rochester and frequently congested major roads are adjacent to both sites. In the same way, the population density was assumed to be similar near both sites suggesting similar impacts of domestic emissions. However, some differences in the strength of stationary point sources can be expected since the two sites are at differing distances and directions from the two large power plants. Effects of site change may be expected around 2004 for species mainly linked to the stationary sources, such as SO_2 and sulfate.
- The shift in ozone monitoring from the pre-2004 east side site to the new one represented a relatively short distance, but the change in local environment from residential to a location much closer to major highways (I-490, I-590 and NY 96) suggests the potential for differences resulting from higher NO concentrations at the newer location. Unfortunately, NO was not measured until later in 2010 so direct comparisons are not possible.
- There were changes in the chemical speciation samplers and the analytical protocols. Three different samplers and two different OC/EC analytical protocols were utilized. Table 1 summarizes the sampling and analytical protocols used over the period of 2001 to 2015 at the Rochester sites. Differences between the EC/OC methods and their results are discussed in multiple reports (Bae et al., 2009; Cheng et al., 2011a, 2011b; Chow et al., 2001, 2004, 2007; Malm et al., 2011; Watson et al., 2005). Good agreement has been reported for total carbon (TC = EC + OC) using the two protocols. However, significant differences particularly in EC are commonly observed among the different EC/OC methods. The carbonaceous fractions are linked to the different temperature steps and optical methods for correcting for OC pyrolysis. For this study, the conversion method proposed by Bae et al. (2009) was applied to estimate NIOSH-like EC/OC from the IMPROVE EC/OC data.

2.4. Statistical methods

Significant upward or downward trends from 2001 through 2015 related to different air pollution species were determined with a nonparametric method based on Mann-Kendall with Thiel-Sen slope (Aguilar et al., 2007; Sen, 1968; Theil, 1992; Visser et al., 2007). Thiel-Sen is a robust regression technique that is insensitive to outliers and provides the median slope from all slopes calculated from all possible pairs of values. Further, a piecewise trend analysis was performed using a three-section linear regression.

To identify the source locations of transported PM (SO_2 emissions), a trajectory ensemble method named Potential Source Contribution Function (PSCF) (Hopke, 2016) was used to estimate of the conditional probabilities of upwind areas being the source locations of the observed pollutants. To estimate the impact of state-level emissions on $PM_{2.5}$ sulfate concentrations in Rochester, a multiple linear regression was performed with independent variables being aggregated state-level SO_2 emissions and the dependent variable was the Rochester sulfate concentrations. First, an automated stepwise selection process was used with a significance level at 0.05 and a confidence level at 95% (Su et al., 2009). State-level emissions were added one-by-one. The parameter most correlated with model residuals was then selected as the next independent variable, and the process repeats. Each independent variable stays in the model if the significance level is <0.05 and the variance inflation factor (VIF, a check for multi collinearity) with parameters already in the model is <5. In the stepwise selection process, the weakest independent variables are rejected. The process automatically ceases when all the remaining variables reached statistically significant values. After screening the variables, a dummy variable for year which reflects

Table 1
History of sampling and analytical protocols for $PM_{2.5}$ speciation measurements in Rochester, NY.

Site	Period	Sampler	Species	Method
36-055-6001	1/01-3/04	R&P 2300 (Teflon)	Elements	XRF (RTI)
		R&P 2300 (nylon)	Ions	Ion Chromatography (RTI)
		R&P 2300 (quartz)	OC/EC	STN NIOSH TOT
36-055-1007	1/05-10/07	R&P 2300 (Teflon)	Elements	XRF (RTI)
	10/07-12/15	Met One SASS (Teflon)	Elements	XRF (RTI)
	1/05-10/07	R&P 2300 (nylon)	Ions	Ion Chromatography (RTI)
	10/07-12/15	Met One SASS (nylon)	Ions	Ion Chromatography (RTI)
	1/05-10/07	R&P 2300 (quartz)	OC/EC	STN NIOSH TOT
	10/07-4/09	Met One SASS (quartz)	OC/EC	STN NIOSH TOT
	4/09-12/15	URG 3000N	OC/EC	IMPROVE_A TOR + TOT

other variability sources was added to the remained SO_2 emissions data and a multivariate linear regression among the mentioned dependent and independent variables is achieved. The model performance was assessed by coefficient of determination (R^2), and root mean squared errors (RMSE) between the measured and estimated $PM_{2.5}$ concentrations. The RMSE was defined as square root of the mean of the squared errors. The entire mentioned procedures were applied over monthly averages (>75% available data). Data analyses including determination of trends of time-series related to different air pollution species as well as multivariate analysis were done using MATLAB.

3. Results and discussion

3.1. Seasonal, weekly, and daily cycles

Monthly-averaged data were analyzed in the trend analyses. Seasonal average statistics of concentrations and the associated 75th and 99th confidence intervals calculated by bootstrapping the data (n = 200) are reported in Fig. SI3. Typical seasonal cycles with maxima in the coldest months (Nov–Feb) and minima in the warmest period (Jun–Sept) were found for pollutants mainly linked to combustion (CO, SO_2, and DC). Such cycles exist given: (i) increased emissions for domestic heating during the colder months; (ii) lower mixed layer heights and possibly strong thermal inversions during the winter, (iii) generally lower winds speeds and increased precipitation particularly snow that scavenges pollutants in winter, and (iv) reduced atmospheric oxidants in shorter photoperiod months. Similar monthly variations are reported in northeastern U.S. (e.g., Rattigan et al., 2010, 2013; Masiol et al., 2017a). Ozone showed the highest concentrations during the warmest season (April–September), i.e. when the solar radiation is higher and the photochemistry is more active. This pattern agrees well with the total amount of direct and diffuse solar radiation (METSTAT-modeled) retrieved from the National Solar Radiation Database (NSRD) (NREL, 2012) (Fig. SI4). OC and sulfate also exhibit higher concentrations in summer as result of the increased atmospheric oxidants concentrations (mainly ·OH radicals). EC and BC show increased concentrations in the late summer and autumn. Similar patterns of carbonaceous PM are already reported in Rochester (Rattigan et al., 2010, 2013; Wang et al., 2011a, 2011b) and are mainly shaped by: (i) the increased outdoor activity in summer (e.g., barbeques); (ii) the open burning of leaves during late summer-autumn; and (iii) the increased wood burning emissions with the onset of colder periods in autumn. During the coldest months and possible snow cover, there is a preference for using natural gas over wood burning for domestic heating. The nitrate seasonality is related to: (i) its equilibrium properties leading to being predominately gaseous at temperatures over 20 °C (Schaap et al., 2004) and (ii) the decrease in sulfate production in winter and the subsequent increase in the availability of ammonia.

Weekly and daily patterns (Figs. SI5 and SI6, respectively) are strongly linked to the patterns of anthropogenic emissions. CO, BC, and $PM_{2.5}$ concentrations reflect road traffic emissions. They show typical daily cycles with two daily maxima linked to the morning and evening rush hours and a weekly pattern with minima during the weekends. Similar patterns are commonly found in northeastern US, e.g., New Jersey (Roberts-Semple et al., 2012), New York (Rattigan et al., 2010, 2013; Masiol et al., 2017a), as well as in southeastern U.S. (Hidy et al., 2014). Daily ozone concentrations follow the increased solar radiation (more evident in summer). The daily (minima at morning rush hours) and weekly (maxima at weekends) patterns clearly point to the ozone being titrated by NO converting it to NO_2. This "weekend" effect is commonly reported in many locations (e.g., Pires, 2012; Huryn and Gough, 2014; Masiol et al., 2017b). The weekly pattern of SO_2 reflects the decreased road traffic during weekends. The diurnal cycle shows an extended maximum during daytime likely related to industrial emissions.

DC and K^+ (both tracers of biomass burning) increase on the weekends due to the increased domestic wood burning in late fall, winter, and early spring and recreational activities in summer such as fires, barbeques, etc. Similar patterns in Rochester are reported by Wang et al. (2012a, 2012b). No statistically significant weekly patterns were found for sulfate and nitrate (Kruskal Wallis test $p > 0.1$).

3.2. Long-term trends

To explore the long-term trends, Mann-Kendal (M-K) with Sen's slope analyses have been applied. Figs. 1 and 2 and Table SI1 present the M-K results using the monthly average species concentrations from the sampling sites in Rochester from 2001 to 2015. DEC moved the speciation sampler from the downtown site (Main Fire Station) to the current east side site in 2004. There are no speciation network data for April to December 2004.

Trends were determined by season since secondary processes like sulfate formation is strongly depending on the seasonally variable photochemical activity. The seasons are defined as December–February (winter), March–May and September–November (transition), and June–August (summer). The M-K regression analyses for the different seasons are shown in Fig. 2 and Table 2. Within each season, there was still considerable variability. The analyses were then further refined to month by month analysis over the multiple years. Tables SI2 to SI5 and Figs. SI8 and SI19 present the individual monthly average results for January to December. The 2001/2015 trends were generally negative, but positive values were obtained for DC, O_3, and K^+. Piecewise regression confirmed that the trends of some species were not constant during this period, and presented unusual patterns (Fig. SI7).

The monthly average concentrations of EC (2001–2015), OC (2001–2015), BC (2005–2015), and DC (2008–2015) are shown in Figs. 1 and 2. The EC trend had a positive slope from 2001 to 2004 (8.32%/y) and a negative trend (−7.18%/y) from 2005 to 2015. To adjust for seasonal patterns, the concentrations were stratified by season and month (Tables 2, and SI2 to SI5 and Figs. 2 and SI8). Piecewise linear regression showed that EC increased between January 2001 and the end of April 2008 (0.03 μg/m^3/y) followed by a decline (−0.11 μg/m^3/y) between

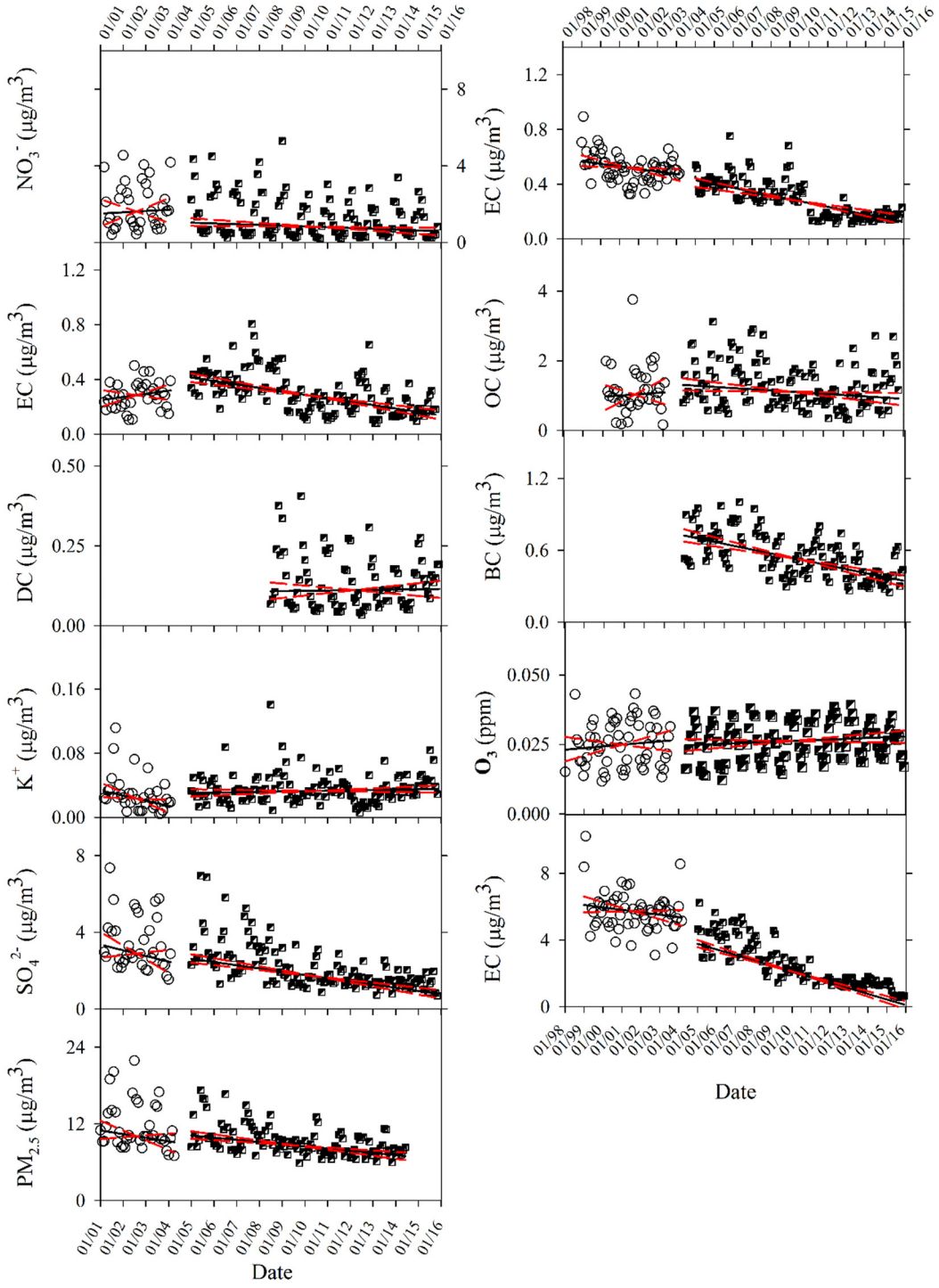

Fig. 1. Trend analysis of all monthly average data of two periods; Mann-Kendall regression, Sen slope (μg/m^3/y) with upper and lower 95% confidence bands in the bracket and Mann-Kendall coefficient.

May 2008 and the end of 2009 and an insignificant downward trend (−0.01 μg/m^3/y) through 2015. This decline may be attributable to reduced truck traffic because of diminished economic activity during this period of economic recession (Fig. 2). The decrease in winter and transition seasonal EC (2005–2015) is about 3 times higher than in summer (Fig. 2, Table 2). Piecewise analysis revealed OC concentrations were rising by 0.10 μg/m^3/y for 2001–2008 and decreasing by −0.41 μg/m^3/y for 2008–2010. From 2011 to 2015, the trend was positive with a moderate slope of 0.05 μg/m^3/y. The trends in OC showed no distinct differences among seasons (Table 2 and Fig. 2). There was an upward trend for the 2001–2004 period (3.64%/y). A downward trend of −0.04 μg/m^3/y (−3.13%/y) was estimated for 2005–2015. Alternatively, Fig. 2 shows some differences in the summer trends (Sen's slope) for OC measured at USEPA site 36-055-6001 (2001–2004) and USEPA site 36-055-1007 (2005–2015). Increased outdoor activity in summer (e.g., barbeque); and the open burning of leaves during late summer may have produced these positive summer trends for OC in 2001 to 2004.

BC trends were similar to EC with a slight upward trend of 0.03 μg/m^3/y from 2005 to 2008 followed by a decline (−0.17 μg/m^3/y) from 2008 to 2010. A very small negative slope (−0.02 μg/m^3/y) was found for 2011–2015. Overall, BC

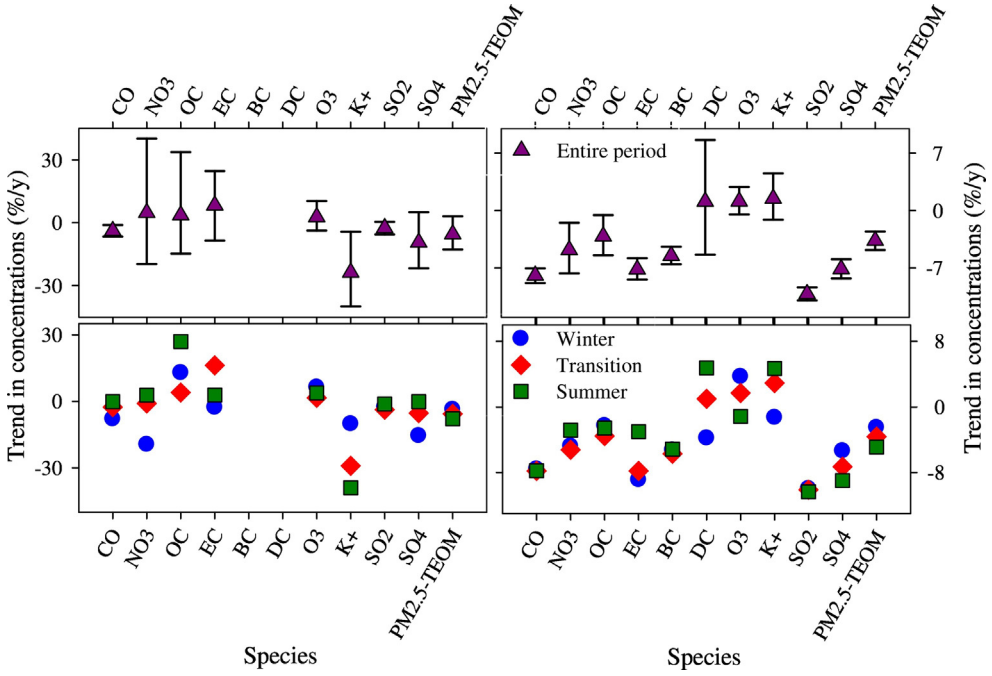

Fig. 2. Trends estimated from Sen's slope for the species measured at (Left) USEPA site 36-055-6001 except O_3, which measured at USEPA site 36-055-1004 prior to May 2004 and (Right) USEPA site 36-055-1007 beginning in May 2004. Error bars indicate upper and lower 95% confidence intervals.

concentrations decreased by a factor of ~5.5%/y over a ten-year period as shown in Figs. 1, 2, and SI7 and Tables SI1 and 2. M-K regression with Sen's slope indicated a slightly increasing trend (1.12%/y or 7.0% overall) for DC for the seven years for which there are data. The DC seasonal cycles add variability to the concentrations unrelated to trends resulting in wider confidence bands as seen in Fig. 2. This added variability increases the uncertainty in the trend estimates. Seasonal investigations show a negative trend for winter with −3.79%/y and increasing values for transition (1%/y) and summer (4.76%/y).

In Fig. 1, the monthly average K^+ concentrations for 2001–2004 and 2005–2015 periods appear to have decreased by −23.7%/y and then increased by 1.46%/y, respectively. Examination of the annual averages for 2001 and 2015 showed an approximately 8% increase in K^+ between these years. K^+ (also a tracer of biomass burning) increased in the 2005–2015 period likely as the result of increased domestic wood burning in late fall, winter, and early spring and recreational activities in summer such as fires, barbeques, etc. (Fig. 2).

Maximal O_3 concentrations are more likely to occur during the warmer months, when favorable meteorological conditions, enhanced photochemistry, and availability of reactive organic precursors are more conducive to O_3 formation (Fig. SI13). O_3 concentrations during the 1999–2015 are generally lower than the NAAQS level of 70 ppb throughout Rochester (Fig. 1). In general, analyses show an upward trend for monthly average O_3 concentrations except for the summer months of 2005–2015 (Figs. 1 and 2 and Table 2). During the winter and transition seasons, increasing trends were found, likely due to decreasing NOx emissions, which leads to decreased titration of ozone.

An upward trend (4.77%/y) for 2001–2004 and a downward slope of ~5%/y for 2005–2015 was obtained for NO_3^-. Winter shows a stronger trend than either the transition or summer seasons for 2001–2015 (Table 1 and Fig. 2). Particulate NO_3^- derives from nitrogen oxides that are emitted from roadway vehicles and space heating with natural gas. The National Low Emission Vehicle (NLEV) program in 2000 and Tier 2 Vehicle controls led to reductions in tailpipe emissions including NO_x. Therefore, the reductions in ambient particle NO_3^-, especially winter 2001–2004, (Table 1 and Fig. 2) may be attributed to the combined impact of the controls on stack and vehicle emissions (Rattigan et al., 2016). Fig. SI14 show the monthly trends in NO_3^- with the highest concentrations in winter and lowest in summer.

Substantial reductions (−81%) in CO concentrations at Rochester were observed between 1999 and 2015. CO does not exhibit a strong seasonal variation and the concentrations dropped ~7.5%/y during the 2005–2015 period. Heavy-duty diesel controls, and more fuel-efficient engines based on 2004 off-road emission rules and changing fuel economy standards have led to substantial reductions in CO emissions in Rochester.

The largest change in concentrations is for SO_2 during 2005 to 2015 (Table SI1). The piecewise regression analysis for 1999 to 2008 showed that SO_2 concentrations declined by −0.50 ppb/y (Fig. SI7). From 2008 to 2010, a decline of −0.82 ppb/y was observed. The change is likely driven by the closing of the 260 MW Russell coal-fired power plant at the end of April 2008, the reduction in on-road diesel fuel sulfur to <15 ppm beginning on October 1, 2006 and reductions in non-road diesel fuel sulfur in 2010. From 2010 to 2015, a slower reduction of −0.20 ppb/y was observed. The other major local SO_2 source is Kodak Park. The SO_2 emissions for Russell and Kodak coal-fired power plants are shown in Fig. SI16. The Russell emissions were substantially higher than Kodak Park. Thus, the reductions in SO_2 are due in part to Russell closure, but changes in other sources such as local truck and railroad traffic likely contributed as the sulfur concentration in diesel fuels was reduced. Fig. SI17 shows that SO_2 has exhibited a clear winter maximum and summer minimum, and the amplitude of this seasonal variation has diminished substantially over the years. This seasonal pattern can be attributed to lower mixed layer heights and wind speeds in winter, and some No. 2 oil combustion for space heating. There were also two large coal-fired power plants in Dunkirk and Buffalo, NY that would contribute to SO_2 concentrations through moderate range (100 to 150 km) transport. These plants have now closed and future studies will permit determination of the effect of these closures on SO_2 and sulfate in Rochester.

Sulfate shows a similar downward trend as SO_2. The largest change occurred between 2008 and 2010 with a −0.7 $\mu g/m^3$/y decrease being observed. The period of 2001–2008 showed a −0.1 $\mu g/m^3$/y decline. After 2010, concentrations changes were small (−0.05 $\mu g/m^3$/y)

Table 2
Statistics—seasonal trends; Sen's slope (concentration/y) with upper and lower 95% confidence bands, Mann-Kendall tau (Mann-Kendall coefficient adjusted for ties) for the measured data at different sampling sites.[a]

Mann-Kendall regression										
	USEPA site 36-055-6001[a] (2001-2004)[b]					USEPA site 36-055-1007 (2005-2015)[c]				
Species	Sen's Slope	Lower band	Upper band	MK tau (p)[d]	Trend (%/y)	Sen's Slope	Lower band	Upper band	MK tau (p)[d]	Trend (%/y)
Winter										
CO	-0.05	-0.08	-0.03	-0.6 (0.001)	-7.94	-0.03	-0.04	-0.02	-0.53 (<0.001)	-7.58
NO_3^-	-0.13	-0.22	-0.05	-0.39 (0.35)	-19.42	-0.13	-0.22	-0.05	-0.39 (0.002)	-4.77
OC	0.14	-0.49	0.79	0.11 (0.75)	12.92	-0.02	-0.07	0.02	-0.16 (0.21)	-2.28
EC	-0.01	-0.19	0.14	-0.06 (0.92)	-2.64	-0.03	-0.04	-0.02	-0.48 (<0.001)	-8.88
BC	-	-	-	-	-	-0.03	-0.04	-0.02	-0.50 (<0.001)	-5.25
DC	-	-	-	-	-	-0.01	-0.02	0.01	-0.19 (0.24)	-3.79
O_3	0.001	1.87×10^{-4}	0.002	0.47 (0.01)	6.4	7.15×10^{-4}	1.70×10^{-4}	0.001	0.31 (0.01)	3.72
K^+	-0.003	-0.03	-0.004	-0.22 (0.47)	-10.15	-4.99×10^{-4}	-1.80×10^{-3}	8.20×10^{-4}	0.10 (0.45)	-1.28
SO_2	-0.16	-0.55	0.14	-0.18 (0.34)	-2.59	-0.42	-0.5	-0.35	-0.73 (<0.001)	-9.97
SO_4^{2-}	-0.36	-0.55	1.02	-0.28 (0.35)	-15.46	-0.11	-0.17	-0.07	-0.45 (<0.001)	-5.35
$PM_{2.5}$-TEOM	-0.32	-1.09	0.58	-0.2 (0.44)	-3.63	-0.21	-0.39	-0.08	-0.41 (0.002)	-2.5
Transition										
CO	-0.01	-0.04	0.003	-0.22 (0.09)	-2.6	-0.03	-0.03	-0.02	-0.51 (<0.001)	-7.8
NO_3^-	-0.04	-0.1	0	-0.18 (0.97)	-0.94	-0.04	-0.1	0.003	-0.15 (0.03)	-5.24
OC	0.04	-0.25	0.35	0.10 (0.60)	3.97	-0.04	-0.08	0.001	-0.17 (0.04)	-3.55
EC	0.04	-0.03	0.09	0.19 (0.29)	16.21	-0.03	-0.04	-0.02	-0.45 (<0.001)	-7.81
BC	-	-	-	-	-	-0.03	-0.05	-0.02	-0.40 (<0.001)	-5.71
DC	-	-	-	-	-	8.66×10^{-4}	-0.007	0.009	0.01 (0.89)	0.99
O_3	4.45×10^{-4}	-0.002	0.002	0.06 (0.67)	1.60	4.11×10^{-4}	-1.32×10^{-4}	8.92×10^{-4}	0.12 (0.17)	1.7
K^+	-0.006	-0.02	0.002	-0.21 (0.20)	-29.06	8.22×10^{-4}	-4.52×10^{-4}	0.002	0.11 (0.24)	2.93
SO_2	-0.19	-0.46	0.08	-0.16 (0.22)	-3.72	-0.29	-0.36	-0.23	-0.74 (<0.001)	-10.11
SO_4^{2-}	-0.15	-0.64	0.19	-0.15 (0.40)	-5.3	-0.16	-0.21	-0.12	-0.48 (<0.001)	-7.29
$PM_{2.5}$-TEOM	-0.62	-1.59	0.19	-0.20 (0.23)	5.66	-0.33	-0.48	-0.22	-0.42 (<0.001)	-3.63
Summer										
CO	-0.001	-0.04	0.05	-0.001 (0.96)	-0.17	-0.03	-0.03	-0.02	-0.55 (<0.001)	-7.8
NO_3^-	-0.01	-0.03	0	-0.23 (0.92)	2.81	-0.01	-0.03	3.79×10-4	-0.23 (0.06)	-2.85
OC	0.4	-0.83	1.24	0.33 (0.25)	26.9	-0.05	-0.13	0.02	-0.17 (0.16)	-2.59
EC	0.01	-0.16	0.2	0.00 (0.92)	2.83	-0.01	-0.02	0	-0.27 (0.03)	-3.01
BC	-	-	-	-	-	-0.04	-0.05	-0.02	-0.46 (<0.001)	-5.16
DC	-	-	-	-	-	0.002	-0.003	0.008	0.14 (0.37)	4.76
O_3	0.001	-0.002	0.004	0.21 (0.32)	3.82	-3.71×10^{-4}	9.60×10^{-4}	1.41×10^{-4}	-0.19 (0.13)	-1.15
K^+	-0.02	-0.04	-0.006	-0.50 (0.08)	-38.97	1.30×10^{-3}	-1.30×10^{-3}	0.003	0.12 (0.31)	4.69
SO_2	-0.06	-0.35	0.27	-0.14 (0.49)	-1.18	-0.31	-0.38	-0.26	-0.80 (<0.001)	-10.35
SO_4^{2-}	-0.01	-1.6	1.23	0.00 (0.92)	-0.17	-0.33	-0.43	-0.25	-0.60 (<0.001)	-8.99
$PM_{2.5}$-TEOM	-1.42	-3.76	2.23	-0.17 (0.60)	-7.87	-0.65	-0.94	-0.35	-0.47 (<0.001)	-4.89

[a] In case of O_3, the sampling site was USEPA site 36-055-1004.
[b] In case of CO, O_3 and SO_2 is from 1999 to 2004.
[c] In case of DC is from 2008 to 2015.
[d] The values in the parenthesis shows the p value.

(Fig. SI7). The monthly averages over the whole period showed consistent downward trends of −9.38%/y (2001–2004) and −7.14%/y (2005–2015). Minimum concentrations were observed in winter and autumn (Fig. SI18).

Fig. 1 and Table SI1 show downward trends of $PM_{2.5}$ TEOM of −5.45 and −3.67%/y for the two periods. Fig. SI7 shows a significant downward trend of approximately −0.82 μg/m^3/y for $PM_{2.5}$ during 2008–2010. For 2001–2008 and 2010–2015, smaller changes (0.34 and −0.21 μg/m^3/y, respectively) were observed. Consistent declines in the monthly mean $PM_{2.5}$ mass were observed since 2001 (5.45 and 3.67%/y). Mann-Kendall trend tests show that these are significant at the 95% confidence interval. For example, monthly mean $PM_{2.5}$ mass ranged from 8 to 17 μg/m^3 in 2001 compared to 3 to 10 μg/m^3 in 2015, a decrease of 5 to 7 μg/m^3 or a 41 to 62% decrease. Thus, $PM_{2.5}$ mass in Rochester has decreased to below the current annual average NAAQS of 12 μg/m^3. Similar decreases were observed for SO_4^{2-} (−65%), BC (−42%), NO_3^- (−37%) and EC (−21%) as major components of $PM_{2.5}$. The exception to these declining trends was OC that increased by 38% during the fifteen years. It is not known why OC is rising, but it can be hypothesized that the reductions in SO_2 and NO_x emissions has resulted in more hydroxyl radicals being available to form additional secondary organic matter along with the increase in residential wood combustion.

3.3. Relationships with upwind SO_2 emissions: regression analyses

Monthly average $PM_{2.5}$ sulfate concentrations in Rochester from January 2001 to December 2015 are shown in Fig. 1. A recurring feature of these data is the annual summer peak. Concentrations are highest during the warm months (April to September) and lowest during the cold (October to March), peaking during June and July. Several studies (Husain et al., 1998; Dutkiewicz et al., 2000 and Husain et al., 2004) showed that the changes in the annual mean SO_4^{2-} concentrations at Whiteface Mountain (a rural background site in north central NYS) and Mayville (a rural background site in southwestern NYS) linearly followed changes in the SO_2 emissions in eight upwind and contiguous states. Data from other networks in the Northeast U.S. have reported similar results (Malm et al., 2002). The relationships between SO_4^{2-} concentrations and regional SO_2 emissions were investigated for the 2001–2015 period by using air parcel back trajectories to identify the likely regions from which the air masses reach Rochester (Zhou et al., 2017). PSCF plots (Fig.

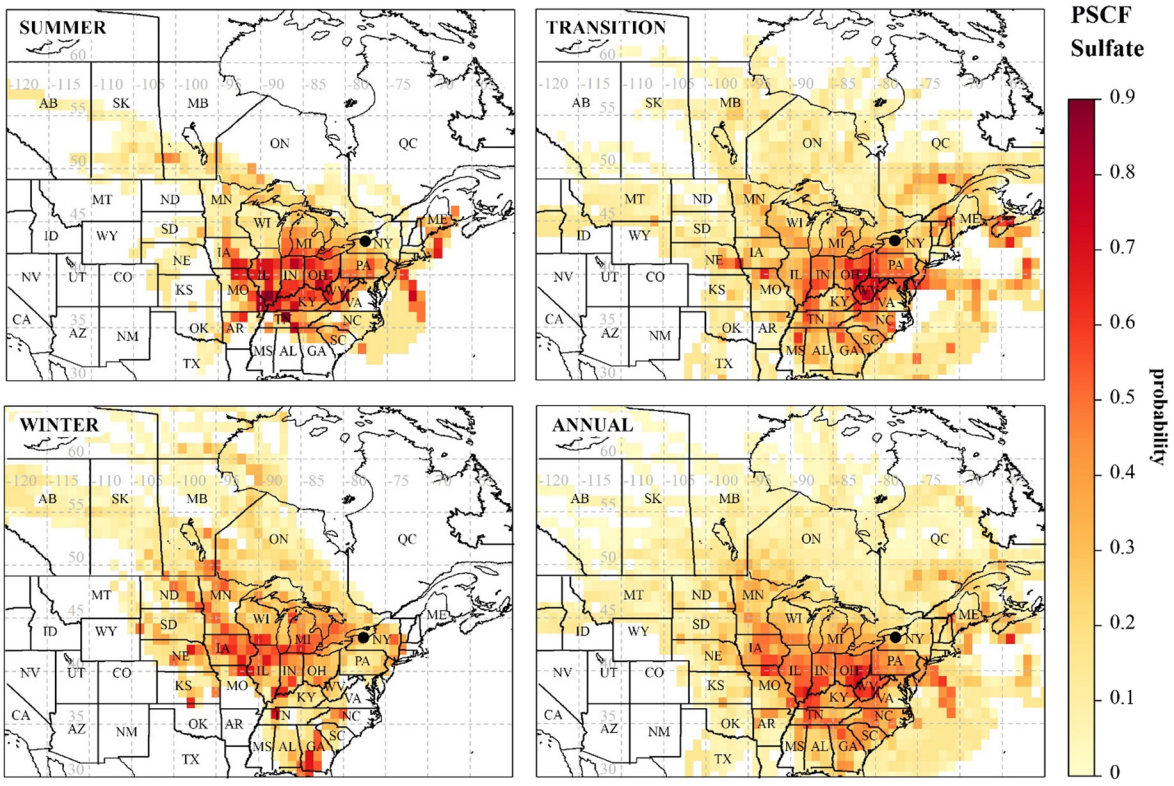

Fig. 3. PSCF for different seasons and entire period.

3) indicate the regions (U.S. and Canada States) with high conditional probabilities for different seasons and the entire period. Fig. 3 was used to identify sixteen states (NY, MI, OH, WI, IA, MN, ND, NE, KS, MO, GA, TN, NC, IN, IL and ON) for winter, fourteen states (MI, NE, IN, IL, MO, OH, PA, KY, WV, VA, NC, GA, TN and MS) for transition, and eleven states (MI, PA, OH, IN, IL, IA, MO, KY, WV, AR and TN) for summer. All of the states were considered in the regression analyses to relate ambient sulfate concentrations with reported aggregate state-wide SO_2 emissions.

The monthly mean SO_4^{2-} in Fig. 1 generally follows the aggregated regional SO_2 emissions with $r = 0.70$ for the included states. This result indicates that changes have generally been fairly homogeneous over the region and it is best to treat these emissions with a screening method. SO_2 emissions of each upwind state were screened using stepwise regressions to maximize correlations (Pearson's r) and minimize Akaike information criterion (AIC). AIC is a metric for choosing among a series of statistical models of the data. It allows for a choice among the models for the one that best fits the data without overfitting or underfitting them. The entered variables had $p < 0.05$, contributed at least 1% to the adjusted R^2, and had correlations <0.6 with variables already in the model (Henderson et al., 2007). Therefore, the variables described above were incorporated into a regression model. All p-values were <0.001 and the signs of all coefficients in the model must be positive. The most important states identified by the variable-screening process were SO_2 emissions of GA for winter, NC for transition, OH for summer and MI and NC for the entire period (Table SI6).

3.4. Final regression model

Considering the variability that may occur in meteorological conditions and the other likely sources of SO_2, the trends of SO_4^{2-} concentrations in Fig. 1 may have affected by systematic changes that are not reflected in the emissions data. For this reason, a dummy variable was added for year (T) in the multivariate regression as follows

$$SO_4^{2-} = aT + b(SO_2)_1 + c(SO_2)_2 + \cdots$$

where $T = 0, 1, 2, \ldots$, year and subscripts refer to regional aggregated SO_2 emissions for state i.

The parameters were estimated using multiple linear regression. The adjusted R^2 and root-mean-square error (RMSE) were used as measures of model performance. Both statistics were stable under leave-one-out cross-validation by iteratively excluding each monitored month from the data, suggesting robust estimates with small outlier influence. Another calculated parameter is selectivity ratio (SR) that provides a simple numerical assessment of the usefulness of each variable in a regression model (Rajalahti et al., 2009). The larger the selectivity ratio, the more useful the given variables are for the prediction:

$$SR_i = \frac{v_{expl,i}}{v_{res,i}}, i = 1, 2, 3\ldots$$

where $v_{expl,i}$ is explained variance by target projection and $v_{res,i}$ is residual variance of each variable (i). The estimated coefficients and their corresponding selectivity ratios of applied variables (states and year) along with their cross-validated errors (RMSECV) for seasons and entire period are summarized in Table 3. For the winter and transition seasons, the best linear fit with SO_4^{2-} concentration was obtained using Georgia and North Carolina emissions, respectively, with higher impact than the year variable. While a reasonable fit was obtained for SO_4^{2-} concentrations in summer using both Ohio emissions and the dummy year variable. Looking more broadly over the upwind region, there is further influence of variables other than SO_2 emission in the summer time. For example, enhanced photochemical activity (higher solar flux and extended daylight hours compared to other seasons) leads to a higher rate of SO_2 oxidation to SO_4^{2-} that can be more transportable over

Table 3
Estimated coefficients using multiple linear regression model for SO_4^{2-} using the original independent variables

Variables	Winter		Transition		Summer		Entire period	
	Beta[a]	SR	Beta	SR	Beta	SR	Beta	SR
T	-0.42	4.28	-0.73	10.29	-1.65	44.19	-0.90	0.02
SO_2 (GA)	0.14	18.16	-	-	-	-	-	-
SO_2 (NC)	-[b]	-	0.34	36.43	-	-	0.19	10.02
SO_2 (OH)	-	-	-	-	0.22	40.32	-	-
SO_2 (MI)	-	-	-	-	-	-	0.33	3.24
RMSECV[c]	5.17 ($R^2 = 0.66$)[d]		7.64 ($R^2 = 0.74$)		11.11 ($R^2 = 0.79$)		10.17 ($R^2 = 0.69$)	

[a] The unit of year's regression coefficient is $\mu g/m^3/y$ and the unit of regression coefficients associated with SO_2 emitted by different states is $\mu g/m^3/10^3$ tons.
[b] – indicates that a statistically significant beta was not obtained for this variable.
[c] The root mean square error leave-one-out validated (RMSECV) is defined as:

$$RMSECV = \sqrt{\frac{\sum_{i=1}^{n}\left(X_{obs,i} - X_{model,i}\right)^2}{n}}$$

where X_{obs} is observed values and X_{model} is modelled values at time i.
[d] Pearson coefficient between the measured SO_4^{2-} and the calculated SO_4^{2-} by MLR.

longer distances than SO_2. Considering the SR of the entire period, North Carolina has more effect than Michigan emissions with neglect impact of year variable. The model predictions exhibit good agreement with measurements across SO_4^{2-} concentrations with R^2 ~0.7.

4. Conclusions

In summary, long-term air pollution quality monitoring with up to 15-year time-series provided optimal opportunities for investigating and understanding the impacts of political action plans in Northeastern America on air quality at Rochester. The main findings can be summarized as follows: 1) significant decreases were observed for most air pollutants, i.e. SO_2 (−86%), SO_4^{2-} (−65%), BC (−42%), NO_3^- (−37%) and EC (−21%). Downward trends were related to the decreases in local and regional emission sources, e.g., the shutting down of a large coal fire plant, fuel sulfur reductions, car-fleet technology improvements, and the 2008 recession; 2) multiple linear regression model identified the states that were major contributors to $PM_{2.5}$ sulfate concentrations in Rochester, NY. Significant impacts of SO_2 emissions from Georgia and North Carolina were found in the winter and transition months, respectively, and from Ohio for the summer. These observations suggest that further reductions in SO_2 emissions would result in a proportional decrease in sulfate concentrations in Rochester and possibly across the northeastern United States.

Acknowledgments

This work was supported by the New York State Energy Research and Development Authority (NYSERDA) under agreement #59802. We want to thank the New York State Department of Environmental Conservation for their help in assessing the Rochester data and providing the black carbon data.

Appendix A. Supplementary data

Supplementary data to this article can be found online at http://dx.doi.org/10.1016/j.scitotenv.2017.09.026.

References

Adam, M., Schikowski, T., Carsin, A.E., Cai, Y., Jacquemin, B., Sanchez, M., Vierkötter, A., Marcon, A., Keidel, D., Sugiri, D., et al., 2015. Adult lung function and long-term air pollution exposure. ESCAPE: a multicentre cohort study and meta-analysis. Eur. Respir. J. 45, 38–50.
Aguilar, J.B., Orban, P., Dassargues, A., Brouyère, S., 2007. Identification of groundwater quality trends in a chalk aquifer threatened by intensive agriculture in Belgium. Hydrogeol. J. 15, 1615–1627.
Bae, M.-S., Schauer, J.J., Turner, J.R., Hopke, P.K., 2009. Seasonal variations of elemental carbon in urban aerosols as measured by two common thermal-optical carbon methods. Sci. Total Environ. 407, 5176–5183.
Bishop, G.A., Stedman, D.H., 2008. A decade of on-road emissions measurements. Environ. Sci. Technol. 42, 1651–1656.
Bishop, G.A., Schuchmann, B.G., Stedman, D.H., Lawson, D.R., 2011. Emission changes resulting from the San Pedro Bay, California ports truck retirement program. Environ. Sci. Technol. 46, 551–558.
Brown-Steiner, B., Hess, P., Chen, J., Donaghy, K., 2016. Black carbon emissions from trucks and trains in the Midwestern and Northeastern United States from 1977 to 2007. Atmos. Environ. 129, 155–166.
Cheng, Y., He, K., Duan, F., Zheng, M., Du, Z., Ma, Y., Tan, J., 2011a. Ambient organic carbon to elemental carbon ratios: influences of the measurement methods and implications. Atmos. Environ. 45, 2060–2066.
Cheng, Y., Zheng, M., He, K., Chen, Y., Yan, B., Russell, A.G., Shi, W., Jiao, Z., Sheng, G., Fu, J., et al., 2011b. Comparison of two thermal-optical methods for the determination of organic carbon and elemental carbon: results from the southeastern United States. Atmos. Environ. 45, 1913–1918.
Chow, J.C., Watson, J.G., Crow, D., Lowenthal, D.H., Merrifield, T., 2001. Comparison of IMPROVE and NIOSH carbon measurements. Aerosol Sci. Technol. 34, 23–34.
Chow, J.C., Watson, J.G., Chen, L.-W.A., Arnott, W.P., Moosmüller, H., Fung, K., 2004. Equivalence of elemental carbon by thermal/optical reflectance and transmittance with different temperature protocols. Environ. Sci. Technol. 38, 4414–4422.
Chow, J.C., Watson, J.G., Chen, L.-W.A., Chang, M.O., Robinson, N.F., Trimble, D., Kohl, S., 2007. The IMPROVE_A temperature protocol for thermal/optical carbon analysis: maintaining consistency with a long-term database. J. Air Waste Manag. Assoc. 57, 1014–1023.
Chow, J.C., Watson, J.G., Chen, L.-W., Rice, J., Frank, N.H., 2010. Quantification of PM 2.5 organic carbon sampling artifacts in US networks. Atmos. Chem. Phys. 10, 5223–5239.
Colette, A., Granier, C., Hodnebrog, Ø., Jakobs, H., Maurizi, A., Nyiri, A., Bessagnet, B., D'Angiola, A., D'Isidoro, M., Gauss, M., et al., 2011. Air quality trends in Europe over the past decade: a first multi-model assessment. Atmos. Chem. Phys. 11, 11657–11678.
Dallmann, T.R., Harley, R.A., 2010. Evaluation of mobile source emission trends in the United States. J. Geophys. Res. Atmos. 115, D14305.
DieselNet, 2017. Nonroad diesel engines. https://www.dieselnet.com/standards/us/nonroad.php, Accessed date: 14 April 2017.
Dillner, A.M., Phuah, C.H., Turner, J.R., 2009. Effects of post-sampling conditions on ambient carbon aerosol filter measurements. Atmos. Environ. 43, 5937–5943.
Duncan, B.N., Lamsal, L.N., Thompson, A.M., Yoshida, Y., Lu, Z., Streets, D.G., Hurwitz, M.M., Pickering, K.E., 2016. A space-based, high-resolution view of notable changes in urban NOx pollution around the world (2005–2014). J. Geophys. Res. Atmos. 121, 976–996.
Dutkiewicz, V.A., Das, M., Husain, L., 2000. The relationship between regional SO 2 emissions and downwind aerosol sulfate concentrations in the northeastern US. Atmos. Environ. 34 (11), 1821–1832.
Environment and Climate Change Canada (ECCC), 2017. Air pollutant emission inventory - online data search. http://www.ec.gc.ca/inrp-npri/donnees-data/ap/index.cfm?lang=En.
Felton, D., 2005. Modifying 50 °C TEOM Data to be More "FRM like" for AQI Reporting Using a Non-linear Correction Based on the Julian Day. 2005. AAAR Meeting, February 7–11, 2005, Atlanta, GA, USA.
Fenger, J., 2009. Air pollution in the last 50 years–from local to global. Atmos. Environ. 43, 13–22.
Franklin, B.A., Brook, R., Pope, C.A., 2015. Air pollution and cardiovascular disease. Curr. Probl. Cardiol. 40, 207–238.
Frost, G.J., McKeen, S.A., Trainer, M., Ryerson, T.B., Neuman, J.A., Roberts, J.M., Swanson, A., Holloway, J.S., Sueper, D.T., Fortin, T., et al., 2006. Effects of changing power plant NOx emissions on ozone in the eastern United States: proof of concept. J. Geophys. Res. Atmos. 111, D12306.

Henderson, S.B., Beckerman, B., Jerrett, M., Brauer, M., 2007. Application of land use regression to estimate long-term concentrations of traffic-related nitrogen oxides and fine particulate matter. Environ. Sci. Technol. 41, 2422–2428.
Hidy, G.M., Blanchard, C.L., Baumann, K., Edgerton, E., Tanenbaum, S., Shaw, S., Knipping, E., Tombach, I., Jansen, J., Walters, J., 2014. Chemical climatology of the southeastern United States, 1999–2013. Atmos. Chem. Phys. 14, 11893–11914.
Hogrefe, C., Lynn, B., Civerolo, K., Ku, J.-Y., Rosenthal, J., Rosenzweig, C., Goldberg, R., Gaffin, S., Knowlton, K., Kinney, P.L., 2004. Simulating changes in regional air pollution over the eastern United States due to changes in global and regional climate and emissions. J. Geophys. Res. Atmos. 109, D22301.
Hopke, P.K., 2016. Review of receptor modeling methods for source apportionment. J. Air Waste Manag. Assoc. 66 (3), 237–259.
Huryn, S.M., Gough, W.A., 2014. Impact of urbanization on the ozone weekday/weekend effect in Southern Ontario, Canada. Urban Clim. 8, 11–20.
Husain, L., Dutkiewicz, V.A., Das, M., 1998. Evidence for decrease in atmospheric sulfur burden in the eastern United States caused by reduction in SO2 emissions. Geophys. Res. Lett. 25 (7), 967–970.
Husain, L., Parekh, P.P., Dutkiewicz, V.A., Khan, A.R., Yang, K., Swami, K., 2004. Long-term trends in atmospheric concentrations of sulfate, total sulfur, and trace elements in the northeastern United States. J. Geophys. Res. Atmos. 109 (D18).
Hyslop, N.P., 2009. Impaired visibility: the air pollution people see. Atmos. Environ. 43, 182–195.
Kasumba, J., Hopke, P.K., Chalupa, D.C., Utell, M.J., 2009. Comparison of sources of submicron particle number concentrations measured at two sites in Rochester, NY. Sci. Total Environ. 407, 5071–5084.
Katsouyanni, K., Samet, J.M., Anderson, H.R., Atkinson, R., Le Tertre, A., Medina, S., Samoli, E., Touloumi, G., Burnett, R.T., Krewski, D., et al., 2009. Air pollution and health: a European and North American approach (APHENA). Res. Rep. Health Eff. Inst. 5–90.
Kim, E., Hopke, P.K., Qin, Y., 2005. Estimation of organic carbon blank values and error structures of the speciation trends network data for source apportionment. J. Air Waste Manag. Assoc. 55, 1190–1199.
Malm, W.C., Schichtel, B.A., Ames, R.B., Gebhart, K.A., 2002. A 10-year spatial and temporal trend of sulfate across the United States. J. Geophys. Res. Atmos. 107 (D22).
Malm, W.C., Schichtel, B.A., Pitchford, M.L., 2011. Uncertainties in PM2. 5 gravimetric and speciation measurements and what we can learn from them. J. Air Waste Manag. Assoc. 61, 1131–1149.
Maricq, M.M., 2007. Chemical characterization of particulate emissions from diesel engines: a review. J. Aerosol Sci. 38, 1079–1118.
Masiol, M., Hopke, P.K., Felton, H.D., Frank, B.P., Rattigan, O.V., Wurth, M.J., LaDuke, G.H., 2017a. Analysis of major air pollutants and submicron particles in New York City and Long Island. Atmos. Environ. 148, 203–214.
Masiol, M., Squizzato, S., Formenton, G., Harrison, R.M., Agostinelli, C., 2017b. Air quality across a European hotspot: spatial gradients, seasonality, diurnal cycles and trends in the Veneto region, NE Italy. Sci. Total Environ. 576, 210–224.
May, A.A., Nguyen, N.T., Presto, A.A., Gordon, T.D., Lipsky, E.M., Karve, M., Gutierrez, A., Robertson, W.H., Zhang, M., Brandow, C., et al., 2014. Gas-and particle-phase primary emissions from in-use, on-road gasoline and diesel vehicles. Atmos. Environ. 88, 247–260.
Maynard, R.L., 2009. Health effects of urban pollution. Air Qual. Urban Environ. 28, 108.
McDonald, B.C., Gentner, D.R., Goldstein, A.H., Harley, R.A., 2013. Long-term trends in motor vehicle emissions in US urban areas. Environ. Sci. Technol. 47, 10022–10031.
Nopmongcol, U., Jung, J., Kumar, N., Yarwood, G., 2016. Changes in US background ozone due to global anthropogenic emissions from 1970 to 2020. Atmos. Environ. 140, 446–455.
National Renewable Energy Laboratory (NREL), 2012. National Solar Radiation Database 1991–2010 Update: User's Manual. NREL Technical Report NREL/TP-5500-54824.
New York State Energy Research and Development Authority (NYSERDA), 2009. Patterns and Trends. New York State Energy Profiles. Albany, NY, pp. 1993–2007.
New York State Energy Research and Development Authority (NYSERDA), 2016. Patterns and Trends, New York State Energy Profiles: 2000-2014. Final Report available from https://www.nyserda.ny.gov/About/Publications/EA-Reports-and-Studies/Patterns-and-Trends.
Parrish, D.D., Singh, H.B., Molina, L., Madronich, S., 2011. Air quality progress in North American megacities: a review. Atmos. Environ. 45, 7015–7025.
Pires, J.C.M., 2012. Ozone weekend effect analysis in three European urban areas. Clean Soil Air Water 40, 790–797.
Pye, H.O.T., Liao, H., Wu, S., Mickley, L.J., Jacob, D.J., Henze, D.K., Seinfeld, J.H., 2009. Effect of changes in climate and emissions on future sulfate-nitrate-ammonium aerosol levels in the United States. J. Geophys. Res. Atmos. 114, D01205.
Rajalahti, T., Arneberg, R., Berven, F.S., Myhr, K.-M., Ulvik, R.J., Kvalheim, O.M., 2009. Biomarker discovery in mass spectral profiles by means of selectivity ratio plot. Chemom. Intell. Lab. Syst. 95 (1), 35–48.
Rattigan, O.V., Felton, H.D., Bae, M.S., Schwab, J.J., Demerjian, K.L., 2010. Multi-year hourly PM 2.5 carbon measurements in New York: diurnal, day of week and seasonal patterns. Atmos. Environ. 44, 2043–2053.
Rattigan, O.V., Civerolo, K., Doraiswamy, P., Felton, H.D., Hopke, P.K., 2013. Long term black carbon measurements at two urban locations in New York. Aerosol Air Qual. Res. 13, 1181–1196.
Rattigan, O.V., Civerolo, K.L., Felton, H.D., Schwab, J.J., Demerjian, K.L., 2016. Long term trends in New York: $PM_{2.5}$ mass and particle components. Aerosol Air Qual. Res. 16, 1191–1205.
Roberts-Semple, D., Song, F., Gao, Y., 2012. Seasonal characteristics of ambient nitrogen oxides and ground–level ozone in metropolitan northeastern New Jersey. Atmos. Pollut. Res. 3, 247–257.
Schaap, M., Spindler, G., Schulz, M., Acker, K., Maenhaut, W., Berner, A., Wieprecht, W., Streit, N., Müller, K., Brüggemann, E., et al., 2004. Artefacts in the sampling of nitrate studied in the "INTERCOMP" campaigns of EUROTRAC-AEROSOL. Atmos. Environ. 38, 6487–6496.
Schwab, J.J., Felton, H.D., Rattigan, O.V., Demerjian, K.L., 2006. New York State urban and rural measurements of continuous PM2. 5 mass by FDMS, TEOM, and BAM. J. Air Waste Manag. Assoc. 56, 372–383.
Seinfeld, J.H., Pandis, S.N., 2016. Atmospheric Chemistry and Physics: From Air Pollution to Climate Change. John Wiley & Sons.
Sen, P.K., 1968. Estimates of the regression coefficient based on Kendall's tau. J. Am. Stat. Assoc. 63, 1379–1389.
Solomon, P.A., Crumpler, D., Flanagan, J.B., Jayanty, R.K.M., Rickman, E.E., McDade, C.E., 2014. US national PM2. 5 chemical speciation monitoring networks—CSN and IMPROVE: description of networks. J. Air Waste Manag. Assoc. 64, 1410–1438.
Straif, K., Cohen, A., Samet, J., 2013. Air Pollution and Cancer: IARC Scientific Publication No. 161. Int. Agency Res. Cancer Lyon Fr.
Su, J.G., Jerrett, M., Beckerman, B.A., 2009. Distance-decay variable selection strategy for land use regression modeling of ambient air pollution exposures. Sci. Total Environ. 407 (12), 3890–3898.
Tagaris, E., Manomaiphiboon, K., Liao, K.-J., Leung, L.R., Woo, J.-H., He, S., Amar, P., Russell, A.G., 2007. Impacts of global climate change and emissions on regional ozone and fine particulate matter concentrations over the United States. J. Geophys. Res. Atmos. 112, D14312.
Theil, H., 1992. A rank-invariant method of linear and polynomial regression analysis. Henri Theil's Contributions to Economics and Econometrics. Springer, pp. 345–381.
U.S. Environmental Protection Agency (USEPA), 2017. Air markets program data. https://ampd.epa.gov/ampd/.
Visser, A., Broers, H.P., Van der Grift, B., Bierkens, M.F.P., 2007. Demonstrating trend reversal of groundwater quality in relation to time of recharge determined by 3H/3He. Environ. Pollut. 148, 797–807.
Wang, Y., Hopke, P.K., Chalupa, D.C., Utell, M.J., 2011a. Effect of the shutdown of a coal-fired power plant on urban ultrafine particles and other pollutants. Aerosol Sci. Technol. 45, 1245–1249.
Wang, Y., Hopke, P.K., Rattigan, O.V., Xia, X., Chalupa, D.C., Utell, M.J., 2011b. Characterization of residential wood combustion particles using the two-wavelength aethalometer. Environ. Sci. Technol. 45, 7387–7393.
Wang, Y., Hopke, P.K., Rattigan, O.V., Chalupa, D.C., Utell, M.J., 2012a. Multiple-year black carbon measurements and source apportionment using Delta-C in Rochester, New York. J. Air Waste Manag. Assoc. 62, 880–887.
Wang, Y., Hopke, P.K., Xia, X., Rattigan, O.V., Chalupa, D.C., Utell, M.J., 2012b. Source apportionment of airborne particulate matter using inorganic and organic species as tracers. Atmos. Environ. 55, 525–532.
Watson, J.G., Chow, J.C., Chen, L.-W.A., 2005. Summary of organic and elemental carbon/black carbon analysis methods and intercomparisons. Aerosol Air Qual. Res. 5, 65–102.
Watson, J.G., Chow, J.C., Chen, L.-W.A., Frank, N.H., 2009. Methods to assess carbonaceous aerosol sampling artifacts for IMPROVE and other long-term networks. J. Air Waste Manag. Assoc. 59, 898–911.
Watt, J., Tidblad, J., Kucera, V., Hamilton, R., 2009. The Effects of Air Pollution on Cultural Heritage. Springer.
WHO, 2016. WHO global urban ambient air pollution database (update 2016). http://www.who.int/phe/health_topics/outdoorair/databases/cities/en/, Accessed date: 26 August 2016.
Zhou, H., Zhou, C., Lynam, M.M., Dvonch, J.T., Barres, J., Hopke, P.K., Cohen, M., Holsen, T.M., 2017. Atmospheric mercury temporal trends in the northeastern United States from 1992 to 2014: are measured concentrations responding to decreasing regional emissions? Environ. Sci. Technol. Lett. 4 (3), 91–97.